Vol 5 (1) (2024)

Measurement, Control, and Automation

Website: https:// mca-journal.org

ISSN 1859-0551

Lyapunov-based design of a model reference adaptive control for half-car active suspension systems

Le-Hoa Nguyen*, Huu-Lap-Truong Nguyen

The University of Danang - University of Science and Technology
**Corresponding author email: nlhoa@dut.udn.vn*

Abstract

This paper proposes a model reference adaptive control (MRAC) design for vehicle active suspension systems with unknown spring stiffness and damping coefficients with the aim of improving the performance of suspension systems. A mathematical model of a half-car active suspension system is first presented, then a reference model of a half-car suspension system that utilizes the skyhook damping concept is proposed. The control law and adaptation laws for the MRAC that guarantee the dynamic responses of the active suspension system follow well the dynamic responses of the reference model, were derived based on the Lyapunov stability criteria. To evaluate the advantages of the proposed reference model as well as the efficiency of the designed MRAC, the dynamic responses of the reference model, passive, and active suspension systems were analyzed and evaluated both in the frequency and time domains. The obtained results demonstrated that the active suspension system with MRAC provides a better performance in terms of the ride comfort and suspension deflection compared with the passive suspension system.

***Keywords**: Suspension system; half-car model; MRAC; Lyapunov stability.*

Symbols

Symbols	Units	Description
$\mathbf{A}_p$, $\mathbf{A}_m$, $\mathbf{B}_p$, $\mathbf{B}_m$, $\mathbf{C}_p$,		Space state matrix
$\mathbf{X}_p$, $\mathbf{X}_m$		State vector
m_p, m_m	kg	Vehicle body mass
I_p, I_m	kg.m^2	Moment inertia
l_f, l_r	m	Distance from front/rear wheel to the center of gravity
k_{fp}, k_{fm}	N/m	Spring stiffness of front/rear suspension
c_{fp}, c_{fm}	N.s/m	Damping coefficient of front/rear suspension
c_{sky}	N.s/m	Skyhook damping coefficient

Abbreviations

MRAC	Model reference adaptive control

1. Introduction

Suspension system is a crucial part of vehicle, its main functions include: 1) to isolate the vehicle chassis from road disturbances (ride comfort) and 2) to keep the tire in contact with the road surface and to support the vehicle's static weight (road holding) [1]. To improve the ride comfort, it is important to attenuate vertical vibrations in the human sensitive frequency range 4 -8 Hz [2, 3] and around the natural frequency of the vehicle body (usually ~ 1.5 Hz) [4, 5]. The ride comfort is usually quantitatively evaluated by the vertical acceleration of the vehicle body. Road holding is related to the abilities of cornering, braking, and traction during maneuver of the vehicle. These abilities depend on the contact forces between the road surface and the vehicle tire [6, 7]. Therefore, to improve the road holding, it is necessary to minimize the tire deflection and suspension deflection variations induced by road irregularities, especially around the resonance frequency of the unsprung mass (~ 10 Hz) [1, 8]. However, ride comfort and road holding are conflicting performance indexes in suspension system control and design [4, 6, 8].

Based on the ability of to be controlled, suspension systems are classified into three categories: passive suspension, semi-active suspension, and active suspension. A passive suspension system consists of fixed-stiffness spring and non-adjustable damper, therefore, it is difficult to achieve a desired performance simultaneously of ride comfort and road holding [9]. Semi-active suspension systems are equipped with adjustable dampers that can provide performance compared with the passive system. However, control forces generated by adjustable dampers depend on the velocity of suspension deflection [6, 8, 10, 11]. In contrast to the passive and semi-active suspension systems, active suspension systems use external (hydraulic, electromagnetic or pneumatic) power actuators to generate independent forces on the suspension system [12]. Consequently, the active suspension system is the most effective way to improve the vehicle suspension performance and various active suspension control techniques have been

Received: 13 August 2023; Accepted: 06 February 2024.

proposed over the past decades [3, 6, 7, 13-22]. In terms of the ride comfort improvement, Erik et al. proposed to use a model predictive control to compensate the influence of actuator limitations on the ride comfort [13]. To enhance the ride comfort in the human sensitive frequency range (4-8 Hz), the H-infinity control technique that aims to minimize H-infinity norm in specific frequency band was introduced by Sun et al. [3]. A comparative study of different model-based control laws for the active quarter car suspension system such as first-order sliding mode control, high-order sliding mode control, integral sliding mode control, PID control, and linear quadratic regulator control was conducted by Shahid and Wei [14]. To overcome the conflict between ride comfort and road holding, a number of control techniques have been presented such as hybrid fuzzy logic control [6], robust-based H-infinity and mu-synthesis control [15], predictive control based on particle swarm optimization algorithm [16], model reference adaptive control for the quarter car model [17-19], optimal control with exponential decay rate [20], etc.

In practical vehicle systems, the performance of suspension system will be degraded by the variations in the system's parameters. For example, changes in suspension damping coefficient that leads to significantly changes in the ride comfort and road holding indexes [21]. However, the control techniques mentioned above cannot guarantee a desired suspension performance under the parameter uncertainties. To address this issue, adaptive control techniques are the most suitable choice. In [22], the authors proposed an adaptive control design for active quarter suspension system, in which the nonlinear spring stiffness and piece-wise damper dynamics are assumed to be unknown. A constrained adaptive backstepping control scheme for the quarter car active suspension model was presented in [23], where the sprung mass is considered as an uncertain parameter. Model reference adaptive control (MRAC) technique has been proposed in many previous studies to control active suspension systems [17-19]. In the work of Sunwoo et al. [17], MRAC technqique was designed to control the quarter car active suspension model where the sprung mass, suspension spring stiffness and suspension damping coefficient were assumed to be unknown. The obtained results show a significant improvement in term of the ride comfort of the proposed active suspension system to compared with the passive system. A variable structure MRAC was also proposed by Mohammadi [18] to control a quarter car active suspension system. In this work, two skyhook dampers were designed for both the sprung mass and unsprung mass of the reference model in order to achive an improvement in ride comfort and rattle suspension space. To deal with non ideal actuator, a tube-based MRAC approach agumented by a disturbance observer was developed by Mousavi et al. [19] for a quarter car active suspension system. However, the MRAC methods mentioned above are restricted on the quarter car model where pitch motion of the vehicle as well as the delay in road disturbance between the front and rear wheels cannot be evaluated.

In this paper, we proposed a MRAC scheme for the half-car active suspension system with fully unknown in spring stiffness and damping coefficients of both front and rear suspensions is proposed. A skyhook damping concept originally proposed by Karnopp et al. [24] is used to develop the reference model of a half-car active suspension. An adaptation scheme based on Lyapunov stability criteria is developed to guarantee that the dynamic responses of the active suspension system follow asymptotically the dynamic responses of the reference suspension system. Performance of the active suspension system (as well as the reference suspension system) are analyzed and compared with the passive suspension system in both the frequency domain and the time domain. This study contributes the literature as follows:

- A conceptual reference model for the half-car suspension system. The performance of the proposed reference model has been proven to be much better than that of the passive model through the dynamic response analysis in both the time and frequency domains.
- An efficient MRAC scheme for the half-car active suspension system. To our best knowledge, no previous studies have applied MRAC to the half-car suspension model. The proposed method can accommodate large variations in the spring stiffness and damping coefficients of the suspension system and the simulation results show significant improvements over the passive suspension system.

2. Mathematical modelling

2.1. Model of a half-car active suspension

In this current study, to simply the control problem under invesitation, the following assumptions are applied:

- The nonlinear dynamics such as nonlinear characteristics of stiffness and damping are ignored.
- The actuator dynamic is not discussed, actuator saturation is also ignored.
- All state variables are accessable.

Based on the above assumptions, a half-car active suspension model is depicted in Figure 1.

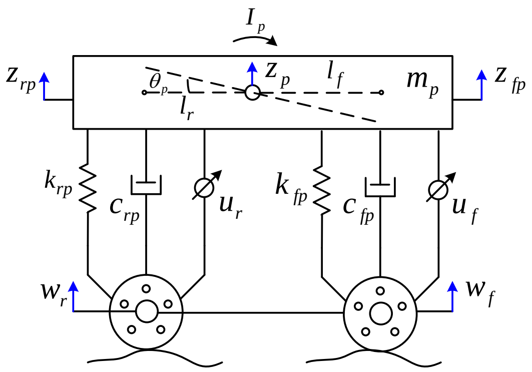

Figure 1: The half-car active suspension model.

The parameters involved include: the mass of vehicle body is m_p, the mass moment of inertia for the vehicle body is I_p, the spring stiffness of the front/rear suspensions are k_{fp} and k_{rp}, respectively, the damping coefficients of the front/rear suspensions are c_{fp} and c_{rp}, respectively, the distances of the front/rear suspension location, with reference to the center of gravity of the vehicle body are l_f and l_r, respectively. Let z_{fp} and z_{rp} be the vertical displacements of the vehicle body at the front/rear suspension locations, respectively. Let w_f and w_r are the vertical displacements of the front/rear wheels, respectively. The vertical displacement and the rotary angle of the vehicle body at the center of gravity are denoted as z_p and θ_p, respectively.

The equations of motion for the vehicle body are given by

$$\begin{aligned} m_p\ddot{z}_p &= -k_{rp}\left(z_{rp}-w_r\right)-c_{rp}\left(\dot{z}_{rp}-\dot{w}_r\right)+u_r \\ &\quad -k_{fp}\left(z_{fp}-w_f\right)-c_{fp}\left(\dot{z}_{fp}-\dot{w}_f\right)+u_f, \end{aligned} \tag{1}$$

$$\begin{aligned} I_p\ddot{\theta}_p &= -\left[k_{rp}\left(z_{rp}-w_r\right)+c_{rp}\left(\dot{z}_{rp}-\dot{w}_r\right)-u_r\right]l_r \\ &\quad +\left[k_{fp}\left(z_{fp}-w_f\right)+c_{fp}\left(\dot{z}_{fp}-\dot{w}_f\right)-u_f\right]l_f. \end{aligned} \tag{2}$$

and the constraints are as follows

$$z_{rp} = z_p + l_r\theta_p, \tag{3}$$

$$z_{fp} = z_p - l_f\theta_p. \tag{4}$$

where u_r and u_f are the control force exerted by controllable actuators at the front/rear suspensions, respectively. In this paper, it is assumed that the exact values of these parameters k_{fp}, k_{rp}, c_{fp}, and c_{rp} are unknown. It is also assumed that there is no limitation on exerting the control forces of the actuators. By defining state variables as $x_{1p} = z_{rp} - w_r$, $x_{2p} = z_{fp} - w_f$, $x_{3p} = \dot{z}_p$, and $x_{4p} = \dot{\theta}_p$, the equations of motion (1)-(2) can be expressed in the state space equation as follows

$$\dot{\mathbf{X}}_p = \mathbf{A}_p\mathbf{X}_p + \mathbf{B}_p\mathbf{v} + \mathbf{C}_p\mathbf{u}, \tag{5}$$

where $\mathbf{v} = \left[\dot{w}_r \quad \dot{w}_f\right]^T$, $\mathbf{u} = \left[u_r \quad u_f\right]^T$, and the matrices $\mathbf{A}_p$, $\mathbf{B}_p$, and $\mathbf{C}_p$ are obtained as follows:

$$\mathbf{A}_p = \begin{bmatrix} 0 & 0 & 1 & l_r \\ 0 & 0 & 1 & -l_f \\ -\dfrac{k_{rp}}{m_p} & -\dfrac{k_{fp}}{m_p} & -\dfrac{c_{rp}+c_{fp}}{m_p} & \dfrac{c_{fp}l_f - c_{rp}l_r}{m_p} \\ -\dfrac{k_{rp}l_r}{I_p} & \dfrac{k_{fp}l_f}{I_p} & \dfrac{c_{fp}l_f - c_{rp}l_r}{I_p} & -\dfrac{c_{rp}l_r^2 + c_{fp}l_f^2}{I_p} \end{bmatrix},$$

$$\mathbf{B}_p = \begin{bmatrix} -1 & 0 \\ 0 & -1 \\ \dfrac{c_{rp}}{m_p} & \dfrac{c_{fp}}{m_p} \\ \dfrac{c_{rp}l_r}{I_p} & -\dfrac{c_{fp}l_f}{I_p} \end{bmatrix}, \quad \mathbf{C}_p = \begin{bmatrix} 0 & 0 \\ 0 & 0 \\ \dfrac{1}{m_p} & \dfrac{1}{m_p} \\ \dfrac{l_r}{I_p} & -\dfrac{l_f}{I_p} \end{bmatrix}.$$

2.2. Proposed reference model of a half-car suspension system

In order to specify the desired performance of ride quality of the suspension system, a skyhook damping system was chosen as the reference model. A skyhook damping model was originally introduced by Karnopp et al. [24]. In this work, to suppress the vibrations of the vehicle body against road disturbances, an inertial damper is connected between the vehicle body and the stationary sky. Based on this concept, a skyhook damping model for a half-car suspension system is proposed in Figure 2.

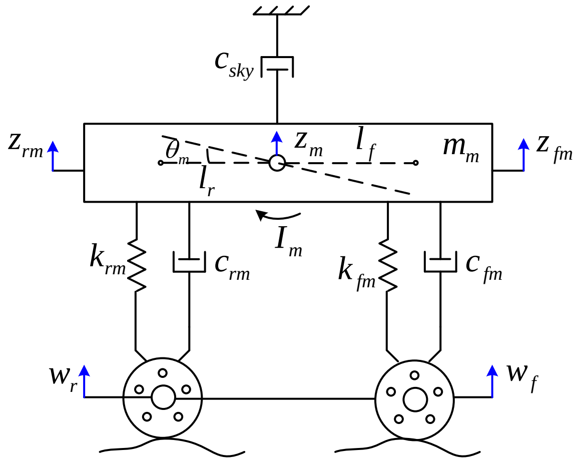

Figure 2: The proposed reference half-car model.

The system's parameters include: the spring stiffness of the front and rear suspensions k_{fm} and k_{rm}, respectively, the damping coefficients of the front and rear suspensions c_{rm} and c_{fm}, respectively, the skyhook damping coefficient c_{sky}, the mass moment of inertia for the vehicle body I_m, and the mass of the vehicle body m_m.

The equations of motion for this model are given by

$$\begin{aligned} m_m\ddot{z}_m &= -k_{rm}\left(z_{rm}-w_r\right)-c_{rm}\left(\dot{z}_{rm}-\dot{w}_r\right) \\ &\quad -k_{fm}\left(z_{fm}-w_f\right)-c_{fm}\left(\dot{z}_{fm}-\dot{w}_f\right)-c_{sky}\dot{z}_m, \end{aligned} \tag{6}$$

$$\begin{aligned} I_m\ddot{\theta}_m &= -\left[k_{rm}\left(z_{rm}-w_r\right)+c_{rm}\left(\dot{z}_{rm}-\dot{w}_r\right)\right]l_r \\ &\quad +\left[k_{fm}\left(z_{fm}-w_f\right)+c_{fm}\left(\dot{z}_{fm}-\dot{w}_f\right)\right]l_f. \end{aligned} \tag{7}$$

and the constraints are

$$z_{rm} = z_m + l_r\theta_m, \tag{8}$$

$$z_{fm} = z_m - l_f\theta_m. \tag{9}$$

As before, we also define the state variables as $x_{1m} = z_{rm} - w_r$, $x_{2m} = z_{fm} - w_f$, $x_{3m} = \dot{z}_m$, and $x_{4m} = \dot{\theta}_m$, the state space equation is obtained as follows:

$$\dot{\mathbf{X}}_m = \mathbf{A}_m\mathbf{X}_m + \mathbf{B}_m\mathbf{v}, \tag{10}$$

where the matrices $\mathbf{A}_m$ and $\mathbf{B}_m$ are given by

$$\mathbf{A}_m = \begin{bmatrix} 0 & 0 & 1 & l_r \\ 0 & 0 & 1 & -l_f \\ -\dfrac{k_{rm}}{m_m} & -\dfrac{k_{fm}}{m_m} & -\dfrac{c_{sky}+c_{rm}+c_{fm}}{m_m} & \dfrac{c_{fm}l_f - c_{rm}l_r}{m_m} \\ -\dfrac{k_{rm}l_r}{I_m} & \dfrac{k_{fm}l_f}{I_m} & \dfrac{c_{fm}l_f - c_{rm}l_r}{I_m} & -\dfrac{c_{fm}l_f^2 + c_{rm}l_r^2}{I_m} \end{bmatrix},$$

$$\mathbf{B}_m = \begin{bmatrix} -1 & 0 \\ 0 & -1 \\ \dfrac{c_{rm}}{m_m} & \dfrac{c_{fm}}{m_m} \\ \dfrac{c_{rm}l_r}{I_m} & -\dfrac{c_{fm}l_f}{I_m} \end{bmatrix}.$$

3. Design of an MRAC controller

The goal of the controller is to bring the state variables of the active suspension system (plant) $\mathbf{X}_p$ described by (5) asymptotically approach the corresponding state variables of the reference system $\mathbf{X}_m$ described by (10) in a short time. In order to achieve that goal, an MRAC method was used. In MRAC algorithm, the controller's parameters are adjusted based on the error between the desired responses of the reference model $\mathbf{X}_m$ and that obtained by the plant model $\mathbf{X}_p$. To ensure the controller's parameters converge to the ideal values that cause the plant's responses to match the responses of the reference model, a Lyapunov stability method was used. In this paper, all state variables as well as the vertical velocities of the wheels are assumed to be accessible.

3.1. Dynamics of error

Let choose the control law as follows:

$$\mathbf{u} = \mathbf{K}_x \mathbf{X}_p + \mathbf{K}_v \mathbf{v}, \tag{11}$$

where $\mathbf{K}_x$ and $\mathbf{K}_v$ are adjustable gain matrices. They are specified as matrices of size (2x4) and (2x2), respectively.
Substituting (11) into (5) yields

$$\dot{\mathbf{X}}_p = \left(\mathbf{A}_p + \mathbf{C}_p \mathbf{K}_x\right)\mathbf{X}_p + \left(\mathbf{B}_p + \mathbf{C}_p \mathbf{K}_v\right)\mathbf{v}. \tag{12}$$

It is obvious that, there would be exist a set of unknown constant gains $\mathbf{K}_x^*$ and $\mathbf{K}_v^*$ such that

$$\mathbf{A}_p + \mathbf{C}_p \mathbf{K}_x^* = \mathbf{A}_m, \tag{13}$$

$$\mathbf{B}_p + \mathbf{C}_p \mathbf{K}_v^* = \mathbf{B}_m. \tag{14}$$

Define the error between the states of the plant model and that of the reference model as

$$\mathbf{e} = \mathbf{X}_p - \mathbf{X}_m. \tag{15}$$

By considering (10) and (12), the dynamics of error yields

$$\dot{\mathbf{e}} = \mathbf{A}_m \mathbf{e} + \left(\mathbf{A}_p - \mathbf{A}_m\right)\mathbf{X}_p + \left(\mathbf{B}_p - \mathbf{B}_m\right)\mathbf{v} + \mathbf{C}_p \mathbf{u}. \tag{16}$$

Using (11), (13), and (14), the dynamics of error is rewritten as follows

$$\dot{\mathbf{e}} = \mathbf{A}_m \mathbf{e} + \mathbf{C}_p \boldsymbol{\Psi} \mathbf{X}_p + \mathbf{C}_p \boldsymbol{\Phi} \mathbf{v}. \tag{17}$$

where $\boldsymbol{\Psi}$ and $\boldsymbol{\Phi}$ are defined as: $\boldsymbol{\Psi} = \mathbf{K}_x - \mathbf{K}_x^*$ and $\boldsymbol{\Phi} = \mathbf{K}_v - \mathbf{K}_v^*$. They are unknown but adjustable gain error matrices.

3.2. Lyapunov stability and adaptation laws

In order to derive parameter adjustment laws, we introduce a Lyapunov function as follows:

$$V = \mathbf{e}^T \mathbf{P} \mathbf{e} + \mathrm{tr}\left(\boldsymbol{\Psi} \mathbf{G}_1^{-1} \boldsymbol{\Psi}^T\right) + \mathrm{tr}\left(\boldsymbol{\Phi} \mathbf{G}_2^{-1} \boldsymbol{\Phi}^T\right) \geq 0, \tag{18}$$

where $\mathrm{tr}(\cdot)$ is the trace of matrix operation, $\mathbf{G}_1$ and $\mathbf{G}_2$ are the adaptation gain matrices of size (4x4) and (2x2), respectively. They are asymmetric and positive definite. Derivative of V along the error, we have

$$\dot{V} = \dot{\mathbf{e}}^T \mathbf{P} \mathbf{e} + \mathbf{e}^T \mathbf{P} \dot{\mathbf{e}} + 2\mathrm{tr}\left(\boldsymbol{\Psi} \mathbf{G}_1^{-1} \dot{\boldsymbol{\Psi}}^T\right) + 2\mathrm{tr}\left(\boldsymbol{\Phi} \mathbf{G}_2^{-1} \dot{\boldsymbol{\Phi}}^T\right). \tag{19}$$

Substituting (17) into (19), yields

$$\begin{aligned} \dot{V} &= \mathbf{e}^T\left(\mathbf{A}_m^T \mathbf{P} + \mathbf{P}\mathbf{A}_m\right)\mathbf{e} + 2\mathbf{e}^T \mathbf{P} \mathbf{C}_p \boldsymbol{\Psi} \mathbf{X}_p \\ &\quad + 2\mathbf{e}^T \mathbf{P} \mathbf{C}_p \boldsymbol{\Phi} \mathbf{v} + 2\mathrm{tr}\left(\boldsymbol{\Psi} \mathbf{G}_1^{-1} \dot{\boldsymbol{\Psi}}^T\right) + 2\mathrm{tr}\left(\boldsymbol{\Phi} \mathbf{G}_2^{-1} \dot{\boldsymbol{\Phi}}^T\right). \end{aligned} \tag{20}$$

Let choose $\mathbf{P}$ as an asymmetric, positive definite matrix and a unique solution of the following equation

$$\mathbf{A}_m^T \mathbf{P} + \mathbf{P} \mathbf{A}_m = -\mathbf{Q}, \tag{21}$$

where $\mathbf{Q}$ is a symmetric, positive definite matrix, and to be specified by the user.
Substituting (21) into (20), we obtained

$$\begin{aligned} \dot{V} &= -\mathbf{e}^T \mathbf{Q} \mathbf{e} + 2\mathbf{e}^T \mathbf{P} \mathbf{C}_p \boldsymbol{\Psi} \mathbf{X}_p + 2\mathbf{e}^T \mathbf{P} \mathbf{C}_p \boldsymbol{\Phi} \mathbf{v} \\ &\quad + 2\mathrm{tr}\left(\boldsymbol{\Psi} \mathbf{G}_1^{-1} \dot{\boldsymbol{\Psi}}^T\right) + 2\mathrm{tr}\left(\boldsymbol{\Phi} \mathbf{G}_2^{-1} \dot{\boldsymbol{\Phi}}^T\right). \end{aligned} \tag{22}$$

If we choose $\boldsymbol{\Psi}$ and $\boldsymbol{\Phi}$ such that

$$\dot{\boldsymbol{\Psi}} = -\mathbf{C}_p^T \mathbf{P} \mathbf{e} \mathbf{X}_p^T \mathbf{G}_1, \tag{23}$$

$$\dot{\boldsymbol{\Phi}} = -\mathbf{C}_p^T \mathbf{P} \mathbf{e} \mathbf{v}^T \mathbf{G}_2, \tag{24}$$

then, we have

$$\begin{aligned} 2\mathrm{tr}\left(\boldsymbol{\Psi} \mathbf{G}_1^{-1} \dot{\boldsymbol{\Psi}}^T\right) &= -2\mathrm{tr}\left(\boldsymbol{\Psi} \mathbf{G}_1^{-1} \mathbf{G}_1 \mathbf{X}_p \mathbf{e}^T \mathbf{P} \mathbf{C}_p\right) = -2\mathrm{tr}\left(\boldsymbol{\Psi} \mathbf{X}_p \mathbf{e}^T \mathbf{P} \mathbf{C}_p\right) \\ &= -2\mathrm{tr}\left(\mathbf{e}^T \mathbf{P} \mathbf{C}_p \boldsymbol{\Psi} \mathbf{X}_p\right) = -2\mathbf{e}^T \mathbf{P} \mathbf{C}_p \boldsymbol{\Psi} \mathbf{X}_p. \end{aligned} \tag{25}$$

Similarly, we can write

$$2\mathrm{tr}\left(\boldsymbol{\Phi} \mathbf{G}_2^{-1} \dot{\boldsymbol{\Phi}}^T\right) = -2\mathbf{e}^T \mathbf{P} \mathbf{C}_p \boldsymbol{\Phi} \mathbf{v}. \tag{26}$$

Substituting (25) and (26) into (22), finally, we obtain

$$\dot{V} = -\mathbf{e}^T \mathbf{Q} \mathbf{e} < 0. \tag{27}$$

By the Lyapunov stability theorem [25], conditions (18) and (27) ensure that the state error $\mathbf{e}$, and parameter gain error matrices $\boldsymbol{\Psi}$, $\boldsymbol{\Phi}$ are stable in the sense of Lyapunov. Furthermore, if we choose the matrices $\mathbf{P}$ and $\mathbf{Q}$ as strictly positive definite matrices, then $\mathbf{e}$, $\boldsymbol{\Psi}$, and $\boldsymbol{\Phi}$ will converge asymptotically to zero.
Finally, it is noted that $\dot{\boldsymbol{\Psi}} = \dot{\mathbf{K}}_x$ and $\dot{\boldsymbol{\Phi}} = \dot{\mathbf{K}}_v$, the parameter adjustment laws are obtained as follows:

$$\dot{\mathbf{K}}_x = -\mathbf{C}_p^T \mathbf{P} \mathbf{e} \mathbf{X}_p^T \mathbf{G}_1, \tag{28}$$

$$\dot{\mathbf{K}}_v = -\mathbf{C}_p^T \mathbf{P} \mathbf{e} \mathbf{v}^T \mathbf{G}_2. \tag{29}$$

The controlled system scheme is depicted in Figure 3.

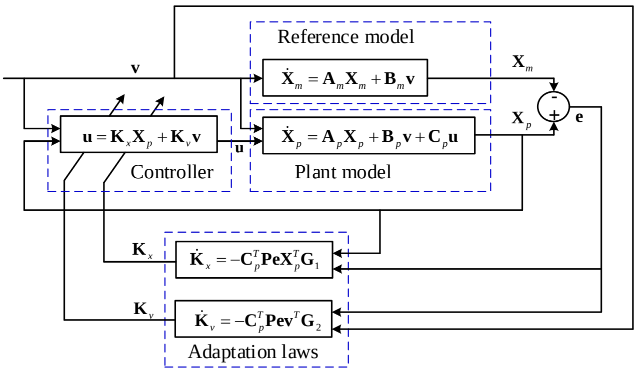

Figure 3: The MRAC scheme of active suspension system.

4. Results and discussions

We will first analyse the performance of the proposed reference system based on the comparison with the performance of the passive suspension system. Note that the half-car passive suspension model can be obtained from (4) by setting control signals $u = 0$. The frequency-domain analysis was performed to investigate the dynamic responses of both the reference and passive models, where the parameters of these two models are given in Table 1. The parameters of the passive system are assumed to be unknown in practice. For simulation, we may select $m_p = m_m$, $I_p = I_m$, $l_{rp} = I_{rm} = l_r$, $l_{fp} = I_{fm} = l_f$, the spring stiffness (k_{fp}, k_{rp}) and the damping coefficients (c_{fp}, c_{rp}) of the front/rear suspension of the passive system are varied up to 30% from these parameters of the reference system, as shown in Table 1. In the following simulations, we consider 6 cases of these parameters of the passive system as follows:

- Case 1: $c_{rp} = c_{rm}$, $c_{fp} = c_{fm}$, $k_{rp} = k_{rm}$, $k_{fp} = k_{fm}$,
- Case 2: $c_{rp} = c_{rm} + 0.3c_{rm}$, $c_{fp} = c_{fm} + 0.3c_{fm}$,
- Case 3: $c_{rp} = c_{rm} - 0.3c_{rm}$, $c_{fp} = c_{fm} - 0.3c_{fm}$,
- Case 4: $k_{rp} = k_{rm} + 0.3k_{rm}$; $k_{fp} = k_{fm} + 0.3k_{fm}$,
- Case 5: $k_{rp} = k_{rm} - 0.3k_{rm}$; $k_{fp} = k_{fm} - 0.3k_{fm}$,
- Case 6: $k_{rp} = k_{rm} + 0.3k_{rm}$, $c_{rp} = c_{rm} - 0.3c_{rm}$.

Table 1: Parameter values of the reference and the passive/active suspension systems

Description	Units	Values	
		Reference model	Passive/active model
Vehicle body mass	kg	$m_m = 850$	$m_p = 850$
Moment inertia of the vehicle body	kg.m^2	$I_m = 1250$	$I_p = 1250$
Distance between the center of gravity and the front suspension	m	$l_f = 1.18$	$l_f = 1.18$
Distance between the center of gravity and the rear suspension	m	$l_r = 1.56$	$l_r = 1.56$
Spring stiffness of the front suspension	N/m	$k_{fm} = 25000$	$k_{fp} = k_{fm} \pm 0.3k_{fm}$
Spring stiffness of the rear suspension	N/m	$k_{rm} = 28000$	$k_{rp} = k_{rm} \pm 0.3k_{rm}$
Damping coefficient of the front suspension	N.s/m	$c_{fm} = 1750$	$c_{fp} = c_{fm} \pm 0.3c_{fm}$
Damping coefficient of the rear suspension	N.s/m	$c_{rm} = 1550$	$c_{rp} = c_{rm} \pm 0.3c_{rm}$
Skyhook damping coefficient	N.s/m	$c_{sky} = 4000$	

Except for the parameters mentioned above, the remaining parameters of the passive system are chosen to be the same as those of the reference system.

The frequency responses of the vehicle body vertical acceleration ($\ddot{z}$) with respect to the derivative of vertical displacements of the front wheel ($\dot{w}_f$) and the rear wheel ($\dot{w}_r$) are shown in Figure 4(a) and Figure 4(b), respectively. It can be seen from Figure 4 that the magnitude of the vehicle body vertical acceleration of the reference system (solid line) is smaller than that of all passive systems (dotted lines) over a large frequency range, especially around the nature frequency of the vehicle body (~ 1.5 Hz) and in the human sensitive frequency range (4-8 Hz) [2]. This also means that the reference system exhibits better ride comfort compared with all passive systems.

Figure 5 shows the frequency responses of the suspension deflection ($z - w$) with respect to the derivative of vertical displacements of the wheel ($\dot{w}$) for the reference system (solid line) and all passive systems (dotted lines). The figures show that the reference system provides a smaller magnitude of the suspension deflection around the natural frequency of the vehicle body ((~ 1.5 Hz) than that of passive systems. In the high frequency region (above 2 Hz), the reference system is observed to have the same magnitude of suspension deflection as passive systems. However, this magnitude is larger than that of passive systems in the low frequency region (below 0.8 Hz).

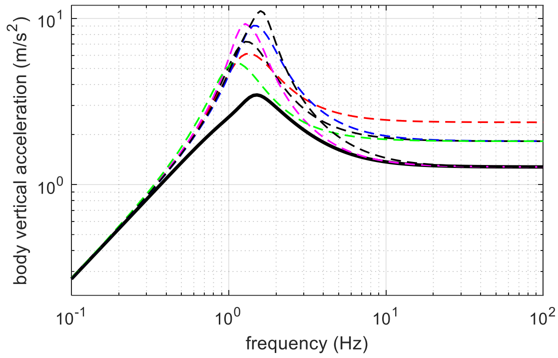

(a)

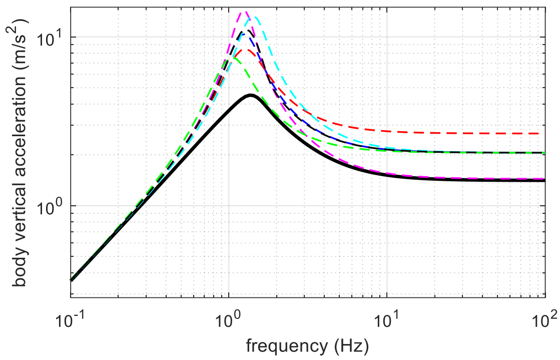

(b)

Figure 4: Frequency responses of vehicle body vertical acceleration with respect to the derivative of vertical displacement of a) front wheel, and b) rear wheel (solid line - reference system, dotted lines – passive system).

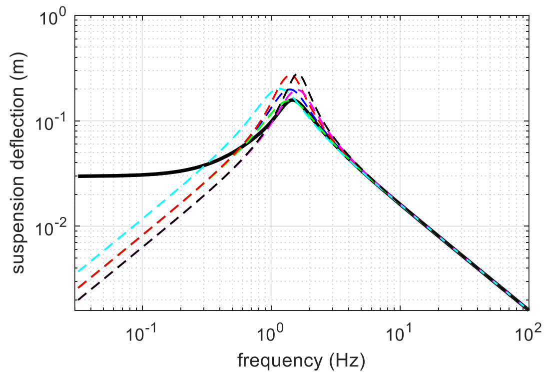

(a)

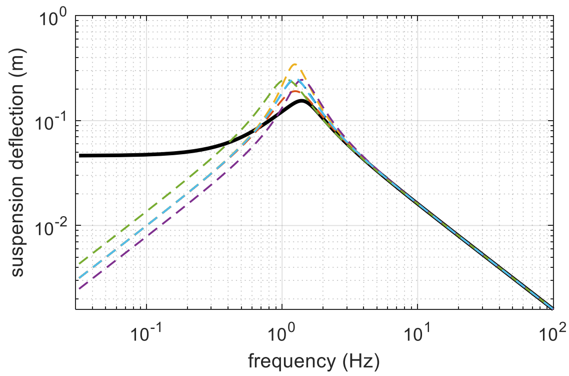

(b)

Figure 5: Frequency responses of suspension deflections at a) the front wheel and b) the rear wheel with respect to the derivative of vertical displacement of the front wheel and rear wheel, respectively, (solid line - reference system, dotted lines – passive system).

Next, the effectiveness of the proposed MRAC scheme for the active suspension system will be examined. To verify the adaptability and robustness of the control system, many different cases that correspond to the variations in the spring stiffness and damping coefficients (Case 1 to Case 6 as mentioned above) of the active system were simulated.

In this simulation, a variable road profile following ISO-2361 was used [26], as follows:

$$\dot{w}(t)+2\pi v n_0 w(t)=\sqrt{G_q(\Omega_0)v}\,\delta(t), \tag{30}$$

where v is a constant vehilce velocity, n_0 is the reference spatial frequency defined as $n_0=0.1$ (cycle/m), $G_q(\Omega_0)$ is the coefficient of road roughness, and $\delta(t)$ is a time-domain white noise. When the vehicle travels at a speed v = 20 m/s under a grade-poor road ($G_q(\Omega_0)=256\times10^{-6}m^3$), the time series of the road disturbance is depicted as in Figure 6.

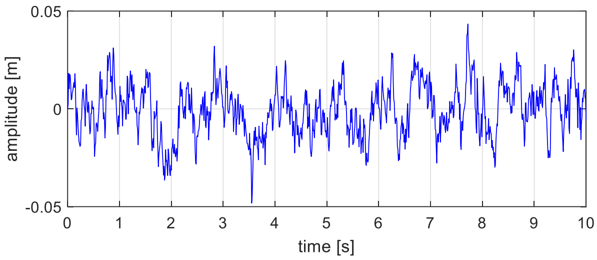

Figure 6: Time course of a grade-poor road.

Since the distance between the front wheel and the rear wheel is $l_f+l_r=2.74$ m, therefore, a time delay of 0.137 seconds was applied to the rear wheel disturbance (i.e., $w_r(t)=w_f(t-0.137)$.

The obtained results show that the trajectory of the active system follows well the trajectory of the reference one. To analyze in more detail, the simulation results for Case 2 (i.e., both damping coefficients of the front and the rear suspension of the active system were increased up to 30% from the nominal values of the reference system) are shown in Figure 7 to Figure 12.

To make sure the convergence of the active suspension's responses to that of the passive suspension system based on the control scheme depicted in Figure 3, the matrices **Q**, **P**, **G**$_1$, **G**$_2$ must be chosen properly (some trail and error is needed). In this simulation, we first chose **Q** as the identity matrix (i.e., $\mathbf{Q}=\mathbf{I}_4$). Solving the Lyapunov equation (21), we obtain

$\mathbf{P}=$[1.931 -0.1715 0.0117 0.005; -0.1715 2.2936 0.0049 -0.0128; 0.0117 0.0049 0.0603 -0.0037; 0.005 -0.0128 -0.0037 0.1056]

Then, after some efforts, the values of matrices **G**$_1$ and **G**$_2$ are selected as

$$\mathbf{G}_1=10^6\times[200\ 10\ 5\ 1;\ 10\ 50\ 6\ 7;\ 5\ 6\ 60\ 10;\ 1\ 7\ 10\ 70],$$

$$\mathbf{G}_2=5\times10^4\times[5\ \ 1;\ 1\ \ 10].$$

Figure 7 shows the errors between states of the active system and the reference model. It is clear that the active suspension system incorporated with MRAC follows well the dynamic response of the reference model. The convergence of the adaptation gains $\mathbf{K}_x$ and $\mathbf{K}_v$ is presented in Figure 8 and Figure 9, respectively.

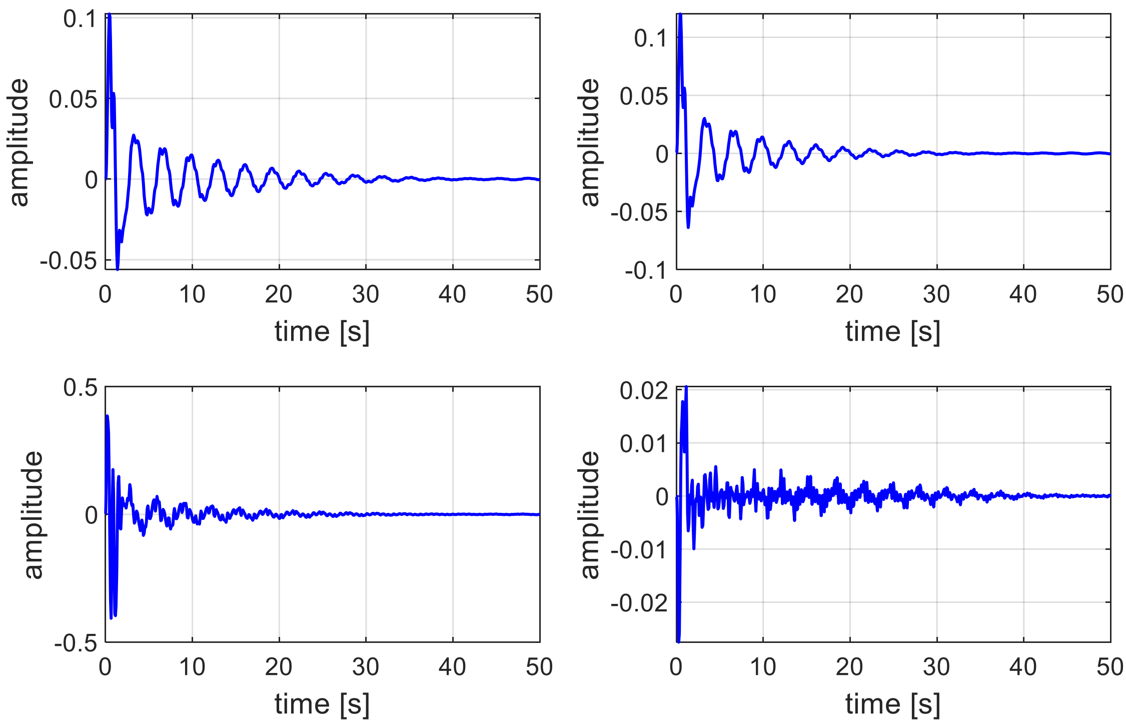

Figure 7: State errors between the reference model and the active system

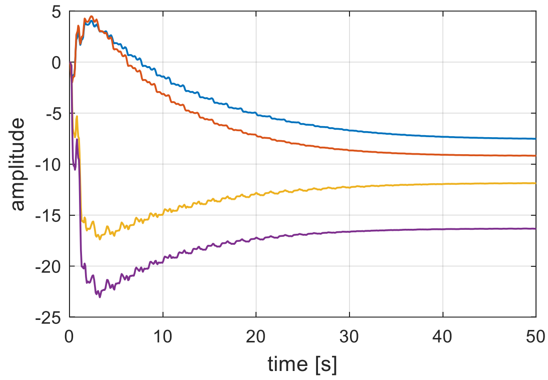

Figure 8: Convergence of the controller gains, $\mathbf{K}_y$.

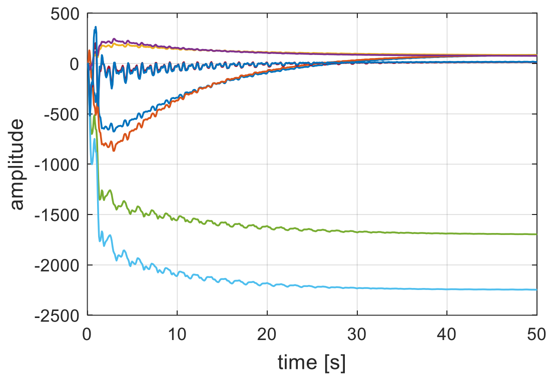

Figure 9: Convergence of the controller gains, $\mathbf{K}_x$.

The time responses of the vehicle body vertical accelerations and pitch angle of the active suspension system (solid line) and the passive system (dotted line) over the road input defined above is depicted in Figure 10 and Figure 11, respectively. It is revealed that the active suspension system has significantly improved the ride comfort compared with the passive system in terms of reduction the magnitude of vehicle body vertical acceleration and pitch angle.

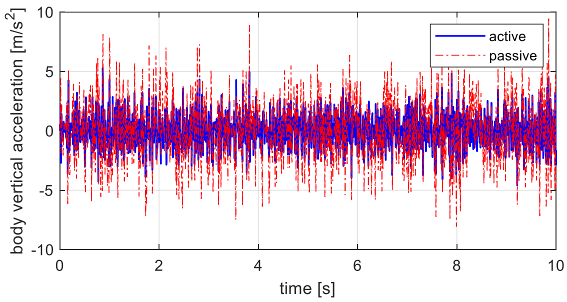

Figure 10: Vehicle body vertical accelerations (solid line – active system, dotted line - passive system).

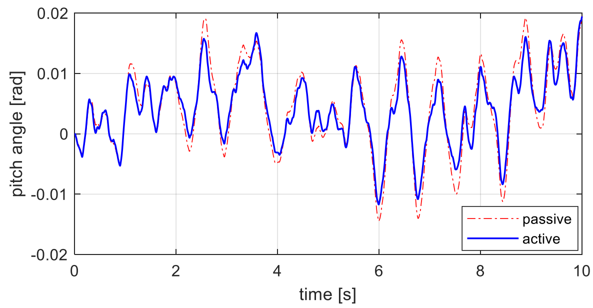

Figure 11: Pitch angle of the vehicle body (solid line – active system, dotted line - passive system).

The comparison of the suspension deflections at the front/rear wheel between the active system and the passive one is shown in Figure 12, in which the solid lines are for the active system and the dotted lines are for the passive system. To quantitatively evaluate the performance of the active suspension system with MRAC, root mean square values of the body vertical acceleration, suspension deflection of both passive and active system were calculated, and the obtained results are shown in Table 2. It can be seen from Table 2 that compared with the passive suspension system, the active system with MRAC can improve the ride comfort in term of vehicle body vertical acceleration by 45.51% and in term of pitch angle by 13.25%. The suspension deflections at the front wheel and the rear wheel are also improved by 18,09% and 34.42%, respectively.

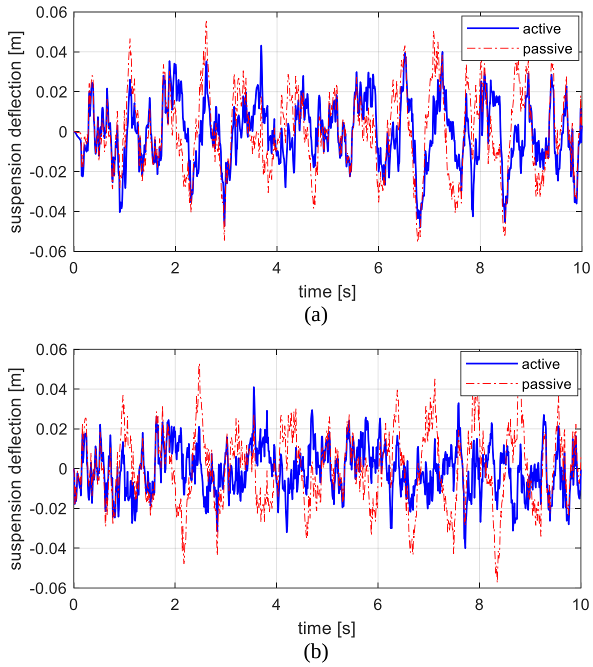

Figure 12: Suspension deflections at a) the rear wheel and b) the front wheel (solid line – active system, dotted line - passive system).

Table 2: Root mean square values of suspension performance indexes.

Suspension performance index	Passive system (Case 2)	Active system with MRAC	Improvement
Body vertical acceleration (m/s^2)	2.6118	1.4232	45.51%
Suspension deflection at front wheel (m)	0.0199	0.0163	18,09%
Suspension deflection at rear wheel (m)	0.0183	0.0120	34,42%
Pitch angle (rad)	0.0083	0.0072	13.25%

5. Conclusion

This paper presented a MRAC for the half-car active suspension systems with unknown spring stiffness and damping coefficients. A reference model for the half-car suspension system was proposed. The Lyapunov stability criteria was utilized for the MRAC design. The responses in the frequency domain show that the reference model provides better performance in terms of the ride comfort and suspension deflection than all the passive suspension systems with spring stiffness and damping coefficients were varied up to 30% from the nominal values of the reference system. The convergence of the dynamic responses of the active suspension system incorporated with MRAC to that of the reference model was verified by numerical simulations in the time domain. The obtained results in the time domain are also revealed that the performance of the active suspension system with MRAC (i.e., vehicle body vertical acceleration, pitch angle, and suspension deflection) has been significantly. To implement the MRAC in practice, futher studies are required to examine realistic phenomena such as nonlinearity, uncertainty, physical limitations, etc. Also, the effects of tire dynamics and full-car model should be considered.

Acknowledgement

This research is funded by the Murata Foundation under the project code: T2022-02-06-MSF.

References

[1] Goodarzi and A. Khajepour, "Vehicle suspension system technology and design," *Synthesis Lectures on Advances in Automotive Technology*, vol. 1, no. 1, pp. i-77, 2017. https://doi.org/10.1007/978-3-031-01494-9

[2] ISO 2631-1, "International organization of standardization. Mechanical vibration and shock – evaluation of human exposure to whole body vibration. Part 1: General requirement," Geneva, 1997. https://www.iso.org/standard/7612.html

[3] W. Sun, H. Gao, and O. Kaynak, "Finite frequency H-infinity control for vehicle active suspension systems," *IEEE Transactions on Control Systems Technology*, vol. 19, no. 2, pp. 416-422, 2011. https://doi.org/10.1109/TCST.2010.2042296

[4] Y. Qin, M. Dong, R. Langari, L. Gu, and J. Guan, "Adaptive hybrid control of vehicle semiactive suspension based on road profile estimation," *Shock and Vibration*, ID 636739, 2015. https://doi.org/10.1155/2015/636739

[5] L.H. Nguyen, K.-S. Hong, and S. Park, "Road frequency adaptive control for semi-active suspension systems," *International Journal of Control, Automation, and System*, vol. 8, no. 5, pp. 1029-1038, 2010. https://doi.org/10.1007/s12555-010-0512-1

[6] M.O. Yatak and F. Sahin, "Ride comfort-road holding trade-off improvement of full vehicle active suspension system by interval type 2 fuzzy control," *Engineering Science and Technology, an International Journal*, vol. 24, no. 1, pp. 259-270, 2021. https://doi.org/10.1016/j.jestch.2020.10.006

[7] W. Li, Z. Xie, P.N. Wong, Y. Cao, X. Hua, and J. Zhao, "Robust nonfragile H-infinity optimum control for active suspension systems with time-varying actuator delay," *Journal of Vibration and Control*, vol. 0, no. 0, pp. 1-18, 2019. https://doi.org/10.1177/1077546319857338

[8] S. Nie, Y. Zhuang, F. Chen, Y. Wang, and S. Liu, "A method to estimate unsprung adverse effect of in-wheel motor-driven vehicles," *Journal of Low Frequency Noise, Vibration and Active Control*, vol. 37, no. 4, pp. 955-976, 2018. https://doi.org/10.1177/1461348418767096

[9] G.D. Shelke, A.C. Mitra, and V.R. Varude, "Validation of simulation and analytical model of nonlinear passive vehicle suspension system for quarter car," *Materials Today: Proceedings*, vol. 5, no. 9, pp. 19294-19302, 2018. https://doi.org/10.1016/j.matpr.2018.06.288

[10] M.M. Rashid, M.A. Hussain, N.A. Rahim, and J.S. Momoh, "Development of semi-active car suspension control system using magneto-rheological damper model," *International Journal of Mechanical and Materials Engineering*, vol. 2, no. 2, pp. 93-108, 2007. https://core.ac.uk/download/pdf/162010461.pdf

[11] K.H. Florean-Aquino, M. Arias-Montiel, J. Linares-Flores, J.B. Mendoza-Larios, and A. Cabrera-Amado, "Modern semi-active control schemes for suspension with MR actuator for vibration attenuation," *Actuators*, vol. 10, no. 2, 2021. https://doi.org/10.3390/act10020022

[12] Y. Zhao and X. Wang, "A review of low-frequency active vibration control of seat suspension systems," *Applied Science*, vol. 9, no. 16, pp. 1-28, 2019. https://doi.org/10.3390/app9163326

[13] E. Enders, G. Burkhard, and N. Munzinger, "Analysis of the influence of suspension actuator limitations on ride comfort in passenger cars using model predictive control," *Actuators*, vol. 9, no. 3, 2020. https://doi.org/10.3390/act9030077

[14] Y. Shahid and M. Wei, "Comparative analysis of different model-based controllers using active vehicle suspension system," *Algorithms*, vol. 13, no. 1, 2020. https://doi.org/10.3390/a13010010

[15] N. Singh, H. Chhabra, and K. Bhangal, "Robust control of vehicle active suspension system" *International Journal of Control and Automation*, vol. 9, no. 4, pp. 149-160, 2016. http://article.nadiapub.com/IJCA/vol9_no4/15.pdf

[16] Q. Zhao and B. Zhu, "Multi-objective optimization of active suspension predictive control based on improved PSO algorithm," *Journal of Vibroengineering*, vol. 21, no. 5, pp. 1388-1404, 2019. https://doi.org/10.21595/jve.2018.19580

[17] M. Sunwoo, K. C. Cheok, and N.J. Huang, "Model reference adaptive control of vehicle active suspension systems," *IEEE Transactions on Industrial Electronics*, vol. 38, no. 3, pp. 217-222, 1991. https://doi.org/10.1109/41.87590

[18] A.K. Mohammadi, "Active control of vehicle active suspension with preview using variable structure model reference adaptive controller," *International Journal of Vehicle Autonomous Systems*, vol. 3, no. 2-4, 253-264, 2005. https://doi.org/10.1504/IJVAS.2005.008236

[19] Y. Mousavi, A. Zarei, I.B. Kucukdemiral, A. Fekih and A. Alfi, "Disturbance observer and tube-based model reference adaptive control for active suspension systems with non-ideal actuators," *IFAC PapersOnline*, vol. 56, no. 2, pp. 1076-1081, 2023. https://doi.org/10.1016/j.ifacol.2023.10.1707

[20] Y.J. Liang and S.L. Wu, "Optimal vibration control for tracked vehicle suspension systems," *Mathematical Problems in Engineering*, vol. 2013, ID. 178354, 2013. https://doi.org/10.1155/2013/178354

[21] S.D. Bruyne, H.V. Auweraer, J. Anthonis, W. Desmet, and J. Swevers, "Preview control of a constrained hydraulic active suspension system," *in 51st IEEE Conference on Decision and Control*, Hawaii, USA, 2012, pp. 4400-4405. https://doi.org/10.1109/CDC.2012.6425847

[22] Y. Huang, J. Na, X. Wu, X. Liu, and Y. Guo, "Adaptive control of nonlinear uncertain active suspension systems with prescribed performance," *ISA Transactions*, vol. 54, pp. 145-155, 2015. https://doi.org/10.1016/j.isatra.2014.05.025

[23] W. Sun, H. Pan, Y. Zhang, and H. Gao, "Multi-objective control for uncertain nonlinear active suspension systems," *Mechatronics*, vol. 24, no. 4, pp. 318-327, 2014. https://doi.org/10.1016/j.mechatronics.2013.09.009

[24] D. Karnopp, M.J. Crosby, and R.A. Harwood, "Vibration control using semi-active force generators," *Journal of Engineering for Industry*, vol. 96, no. 2, pp. 619-626, 1974. https://doi.org/10.1115/1.3438373

[25] H.K. Khalil, *Nonlinear Systems*, 3rd edition, Prentice Hall, 2001.

[26] Y. Zhang, W. Chen, L. Chen, and W. Shangguan, "Non-stationary random vibration analysis of vehicle with fractional damping," *in 13th National Conference on Mechanisms and Machines*, Bangalore, India, 2007, pp. 171-178. https://doi.org/10.1109/ICICTA.2008.348